Timing accuracy and capabilities of XMM-Newton

M. G. F. Kirsch*[a], W. Becker[b], S. Benlloch-Garcia[c], F. A. Jansen[d], E. Kendziorra[c], M. Kuster[b], U. Lammers[d], A. M. T. Pollock[a], F. Possanzini[c], E. Serpell[c], A.Talavera[a]

[a]European Space Agency, Research and Scientific Support Department, Science Operation and Data Systems Division, XMM-Newton Science Operations Centre, P.O. Box 50727, 28080 Madrid, Spain
[b]Max-Planck-Institut für extraterrestrische Physik, Giessenbachstrasse 1, 85784 Garching, Germany
[c]Institut für Astronomie und Astrophysik, Abteilung Astronomie, Sand 1, 72076 Tübingen, Germany
[d]ESA/ESTEC/SCI-SD, P.O. Box 299, NL-2200 AG Noordwijk, The Netherlands
[e]European Space Operations Centre, Robert Bosch Str 5, 64293 Darmstadt, Germany

ABSTRACT

Since December 1999, ESA's large X-ray space observatory XMM-Newton operates in a highly eccentric 48-h orbit which allows for long uninterrupted exposure times. The three payload instruments EPIC, RGS, and OM yield scientific data of high quality and sensitivity. We report here on the current timing capabilities of all three instruments by showing results from analyses on relative and absolute timing. In this context we discuss the process of correlating local onboard event arrival times to terrestrial time frames and present some detailed results from time correlation analyses. This involves investigations on the performance of the onboard quartz oscillator that have been performed. In addition we describe problematic timing data anomalies in the EPIC-pn data and their treatment by the SAS. We show recent examples of timing analyses.

Keywords: XMM-Newton, timing, XTEJ1807-294, Crab

1. INTRODUCTION

Since its launch in December 1999 three instruments operate onboard the European X-ray Multi Mirror observatory XMM-Newton. Three Wolter type 1 telescopes with 58 nested mirror shells focus X-ray photons on the X-ray instruments. In addition a 30 cm Ritchey Chrétien optical telescope is used for optical observations in parallel.

The European Photon Imaging Camera (EPIC) consists of two parts: EPIC-MOS (Metal-Oxide Semi-conductor) and EPIC-pn (p-n-junction). The two EPIC-MOS cameras use front illuminated MOS-CCDs as X-ray detectors while the EPIC-pn camera is equipped with a novel pn-CCD, which has been specially developed for XMM-Newton. EPIC provides spatially resolved spectroscopy over the field-of-view of 30' with a moderate energy resolution. The EPIC camera can be operated in different observation modes related to the different readout in each mode. For a detailed description of the modes see Kendziorra et al. (1997)[1], Kendziorra et al. (1999)[2], Kuster et al. (1999)[3], Ehle et al. (2003)[4]. The RGS spectrometers are designed for high-resolution spectroscopy of bright sources in the energy range from 0.3 to 2.6 keV. With the optical monitor (OM) the field-of-view can be covered simultaneously at visible or UV energies.

All instruments (EPIC, RGS, OM) are able to perform timing analysis to some extent, as discussed below, though the leading instrument for timing analysis is the EPIC-pn camera. Table 1 shows the time resolution for the different instruments and modes. The EPIC-pn camera was designed for imaging, high throughput spectroscopy and timing analysis. EPIC provides high time resolution (Timing: 0.03 ms, Burst: 7 μs) combined with moderate energy resolution (E/dE = 10 to 50) in the nominal energy band from 0.1 to 15 keV. An overview of the current calibration status of the

* Marcus.Kirsch@esa.int; phone +34 91 8131 345; fax +34 91 8131 172

whole EPIC-pn camera is documented in Briel (2003)[5]. The current calibration of the high time resolution modes provides a relative accuracy in the energy of 0.3 % for the Timing Mode and of about 5 % for the Burst Mode over the spectral range from 0.2 to 11 keV (Kirsch et al. 2002)[6].

2. TIME CORRELATION OF XMM-NEWTON

For timing studies it is important to know the absolute photon arrival time in a standard reference system of events that occur onboard the XMM-Newton satellite. XMM-Newton operations are performed in real time from the Mission Operations Centre (MOC) at the European Space Operations Centre (ESOC) in Darmstadt (Germany) via a network of Ground Stations (G/S) located around the Earth to provide almost continuous coverage. Due to this exceptional coverage it is possible to accurately measure the onboard time of the spacecraft (S/C) at all times that it is performing scientific exposures.

Table 1: XMM time resolution in different modes

Mode	Instrument	Time resolution
Extended Full Frame	EPIC-PN	200 ms
Full Frame	EPIC-PN	73.4 ms
Large Window	EPIC-PN	48 ms
Small Window	EPIC-PN	6 ms
Timing	EPIC-PN	0.03 ms
Burst	EPIC-PN	7 micros
Full Frame	EPIC-MOS	2.6 ms
Large Window	EPIC-MOS	0.9 ms
Small Window	EPIC-MOS	0.3 ms
Timing	EPIC-MOS	1.5 ms
Spectroscopy	RGS	0.57 s
HTR	RGS	15 ms
Fast Mode	OM	0.5 s

A standard spacecraft revolution utilises the following sequence of ground stations (from perigee to perigee); Perth, Kourou, Santiago, Perth, Kourou. Occasionally other ground stations can be substituted, for example Santiago for Kourou to allow LEOP (Launch and Early Orbit Phase) support for other missions or VILSPA to cover the short perigee gaps during eclipses.

The following describes the process of correlating onboard events to the Universal Time reference system and presents some results from analysis of this time correlation. As a consequence the performance of the onboard oscillator is determined and discussed.

2.1 Reference Time systems

Time correlation is the process of accurately establishing the relationship between a local time system and a reference time system in order to allow the unequivocal referencing of event arrival times. In the case of XMM-Newton the local time system is known as onboard time (OBT) and the reference system is the Universal Time Co-ordinated (UTC). All events occurring onboard are referenced to the OBT time system.

The OBT local time system is maintained by a crystal oscillator of 2^{23} Hz (approximately 8 MHz) located in the Central Data Management Unit (CDMU). The OBT is initialised at CDMU switch on and continues to run freely from that point. The oscillator temperature is maintained above local ambient temperature with a constant heat supply, however it is important to note that there is no feedback control of the oscillator environment or frequency. The OBT is co-ordinated between onboard subsystems by the CDMU by means of periodical broadcast pulses (BCP) on the spacecraft data bus (OBDH) issued every 2^{23} oscillator cycles, equivalent to one onboard second.

All other spacecraft subsystems maintain a local copy of the OBT and use this information for timing of internal events. The subsystems are required to have their local copy synchronised to the CDMU OBT when they are switched on and to maintain it synchronised using the received BCPs. Additionally, because in some subsystems the local copy is limited to 24 bits of time information, the subsystems are resynchronised every 2^{24} s (about 194 days).

The OBT encoding is standardised as CCSDS (Consultative Committee for Space Data Systems) unsegmented time code with 32 bits of seconds and 16 bits of fractional seconds, i.e. a resolution of approximately 15 μs and a unique identification of more than 130 years.

2.2 From OBT to UTC

XMM-Newton operates with a packeted telemetry stream, where packets from the various subsystems are encapsulated by the CDMU in frames of fixed size and continuously transmitted to ground at a fixed bit rate of 70 kb/s (as measured by the onboard oscillator). Frames are in turn multiplexed in virtual channel frames (VCs), notably VC0 for housekeeping and non-periodic report packets and VC7 for scientific data and idle frames. The instant

of transmission of the first bit of every 16th VC0 frame is timestamped on board in the local OBT system, this happens by means of an hardware mechanism that latches and stores onboard the OBT at the right moment. This time information (in the local time reference OBT) of the event "first bit of the transmission of VC0 frame" is transmitted to ground later in a periodic specific time packet (STSP) before the next 16th VC0 frame occurs again. With a standard XMM-Newton S/C configuration this process repeats approximately at 1/20 Hz. Note that because the timing system is edge triggered the accuracy of the OBT timestamp is not limited by the OBT resolution of 15 µs.

Table 2: Delays in XMM time correlation

Delay	Time in micro sec
CDMU	626.17
G/S Perth	497.33
G/S Kourou	492
G/S Santiago	693
G/S VIL2	460.2
Time of Flight	20000-390000

Each G/S of XMM-Newton is operating in the reference time system UTC and is synchronised through a combination of a local oscillator and a GPS clock with a resolution of 1 µs. On the ground the G/S adds an Earth Received Time stamp (ERT) (in the UTC reference system) to the first bit of each frame it receives. As the time between the transmission and the reception of the VC0 frame is known within a certain accuracy it is possible to correlate the occurrence of the two specific events in the two time references systems (see Figure 1).

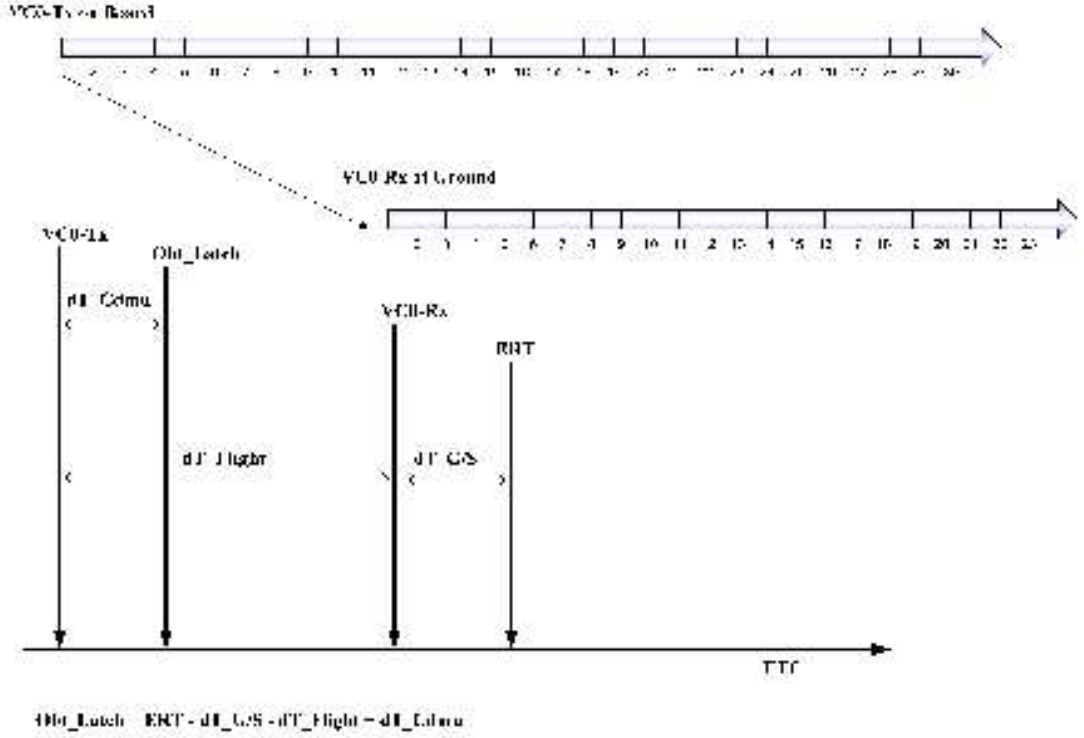

Figure 1: The Timing Information Flow Diagram shows the OBT-UTC time correlation . The formula to correlate OBT and ERT (UTC) is OBT = ERT - dt_GS - dt_FLIGHT + dt_CDMU. The drawing in the lower part shows the correct time model for OBT propagation delay and ERT, where

- VC0-Tx: time event of start transmission of the first bit of VC0 frame used for time correlation
- Obt_Latch: time event of latching on board of OBT
- VC0-Rx: time event at which the first bit of VC0 frame used for time correlation reaches the ground station
- ERT: time event at which the ground station recognises the first bit of VC0 frame and performs the ERT timestamp

To correlate the OBT to UTC it is sufficient to subtract from the ERT the signal travel time from the satellite to the G/S. This time of flight is calculated in real-time by the mission control system at ESOC from knowledge of the predicted orbital position and the G/S location. Additionally the CDMU and G/S timing systems are not infinitely fast and therefore fixed offsets and delays from these components are also considered. To obtain UTC for any OBT it is necessary to fit the pairs of OBT/UTC with a function and use this function to derive the UTC. Due to variations in the OBT oscillator frequency a non-linear fit is required to achieve accurate timing conversion form OBT to UTC over the period of a typical exposure. There is a facility in the Science Analysis System (SAS) to achieve this; the reader is referred to the SAS online documentation. (Package: Observation data file Access Layer library (OAL) at the XMM-Newton Science Operations Centre Home Page http://xmm.vilspa.esa.es).

The final times in the XMM-Newton Observation Data File package (ODF) are offsets in seconds of 1998-01-01T00:00:00 in Terrestrial Time (TT).

2.3 Orbital Information

The Mission Control System (MCS) uses an orbit prediction to calculate the time of flight from S/C to G/S. This file, which is distributed with the ODF, is currently updated every revolution shortly after perigee and thus represents a very good prediction of the forthcoming orbit. The ODF also includes an orbit file that is produced after completion of the relevant revolution and is known as the reconstructed orbit file because the data are reconstructed from the continuous ranging measurements that are made from the G/S to the S/C throughout the revolution.

The difference in the time correlation products as calculated from the orbit prediction are generally the same as those from the reconstructed orbit file, to an accuracy of 30 μs (Serpell et al 2003)[7]. It should be noted that following any anomaly, for example Emergency Safe Attitude Mode (ESAM), there may have been unforeseen changes to the orbit that reduce the accuracy of the prediction. Therefore observers are advised to use the reconstructed orbit file for their final analysis.

2.4 Measured System Performance

Due to the almost continuous coverage of the spacecraft, it is possible to make detailed measurements of the system performance over both long and short time scales.

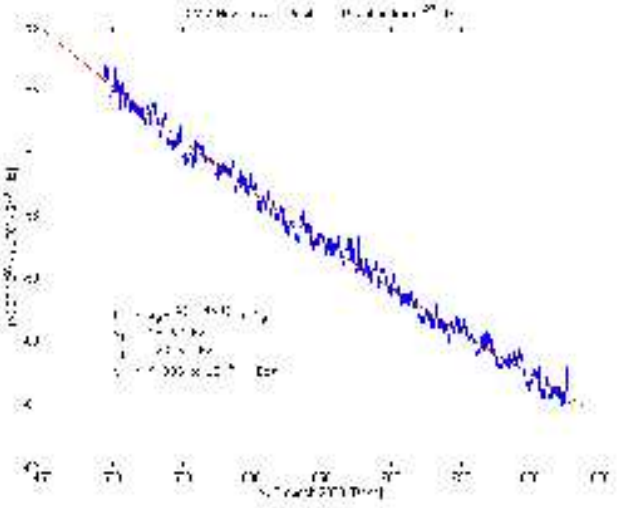

Figure 2: OBT Oscillator Ageing, date is given in days from 1.1.2000

It was observed early in the mission that the relationship between OBT and UTC is not linear, as it would be for a perfect system. This is not surprising, as the crystal oscillator is susceptible to ageing and drift. Ageing is the change in the oscillator frequency over time due to changes in the oscillator mechanism, such as outgassing or adsorption of gas. Drift is the change in oscillator frequency due to external influences, for example thermal and power cycling.

More than two years after launch it has been possible to accurately measure the oscillator performance on both short and long time scales. The long-term variation, on a time scale of years, is dominated by ageing and the short-term variation, on a time scale of hours, is dominated by drift, due to mainly thermal effects.

The frequency of the OBT oscillator was measured for a period of 360 days from day 470 after 01.01.2000. Data was taken from STSP packets at 15-minute intervals. The oscillator frequency was calculated as: $F_{osc} = 65536 * \Delta OBT / \Delta ERT$. Figure 2 shows the frequency compared to the nominal frequency of 2^{25} HZ overlaid with the best fit. The long-term ageing is about 0.016 Hz/day.

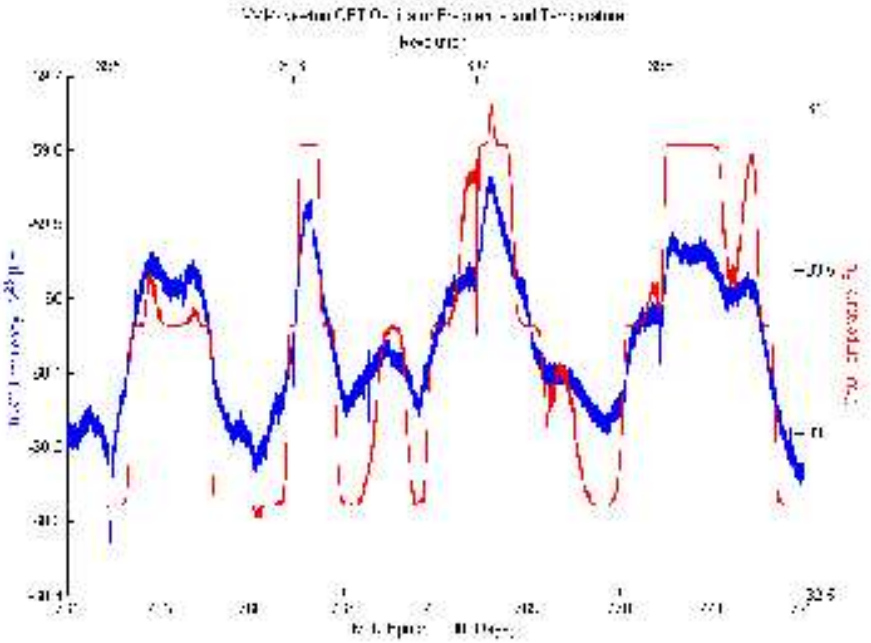

Figure 3: Comparison of OBT Oscillator Drift and Temperature

For short-term analysis the frequency of the OBT oscillator was measured for every STSP for 8 days from day 764 after 01.01.2000. The data was averaged using a running average of width 5 minutes as a low pass filter. The oscillator frequency was calculated as: $F_{osc} = 65536 * \Delta OBT / \Delta ERT$. In addition the oscillator temperature was measured for the same time period and filtered in the same way. Figure 3 shows the variation of the frequency and temperature over the period analysed. There is a clear correlation between temperature and frequency, with a deviation of about ± 0.2 Hz. This variation is in good agreement with the residuals from the long-term ageing measured above. The variation of oscillator frequency with temperature can be modelled with a quadratic polynomial. From the gradient of the polynomial the temperature variation of the oscillator is measured as 0.2537 Hz/ °C at 33 °C.

For both ageing and temperature effects of the OBT oscillator, corrections in the time correlation are in place.

3. EPIC-PN DATA ANOMALIES AND THEIR TREATMENT IN THE SAS

The EPIC-pn event analyser (EPEA) uses the CDMU 1 Hz clock pulse to increment an internal 15 bit wide counter (FTCOARSE) and to reset a 16 bit subsecond (FTFINE) counter which is clocked with 48828.125 Hz. Thus the pn CCD data frames are time stamped with a resolution of 20.48 μs by FTCOARSE/FTFINE pairs. In an ODF they form two columns in the first table of the pn Auxiliary Data File (AUX) which are accessed by SAS in the process of converting frame counters to absolute photon arrival times.

In mid-2000 it was first discovered that the pn AUX data exhibit certain kinds of anomalies whose frequency of occurrence is variable and apparently unrelated to camera mode, observing time or duration. This remains valid until today, i.e. some data sets are completely free of any problems others are heavily affected. Table 3 lists all of the anomalies seen so far. Obviously all these problems need to be corrected for, as otherwise the event times turn out wrong. This is especially critical, as a single shift in FTCOARSE time will cause all subsequent times to be wrongly shifted by the same amount. Pulse profile analyses with a data set that contains a single or multiple undetected and uncorrected such time jumps will then be inconclusive because all photons after the instant of the time jump will be out-of-phase. This can result in a pulse peak broadening, phase shift or the appearance of spurious pulse components. As examples Figure 4 shows the significant influence of time jumps on χ^2-distributions and Z^2-distributions of epoch folding period search. Absolute timing analysis was likely impossible for obvious reasons.

The SAS since the early days can reliably detect and correct for the anomalies with the exception that the detection logic for case 4 in Table 3 sometimes seems to fail with the consequences described above. This, unfortunately, is also true for the public SAS 5.4.1. However we have now been looking in depth at some cases of these jump-detection logic failures and believe to have found a good cure. The anomaly detection/correction algorithm is part of the OAL-3.95 and we have improved it in several ways. With the new SAS release in autumn 2003 we are in a state that all problems are reliably found and corrected and further modifications should not be needed any longer.

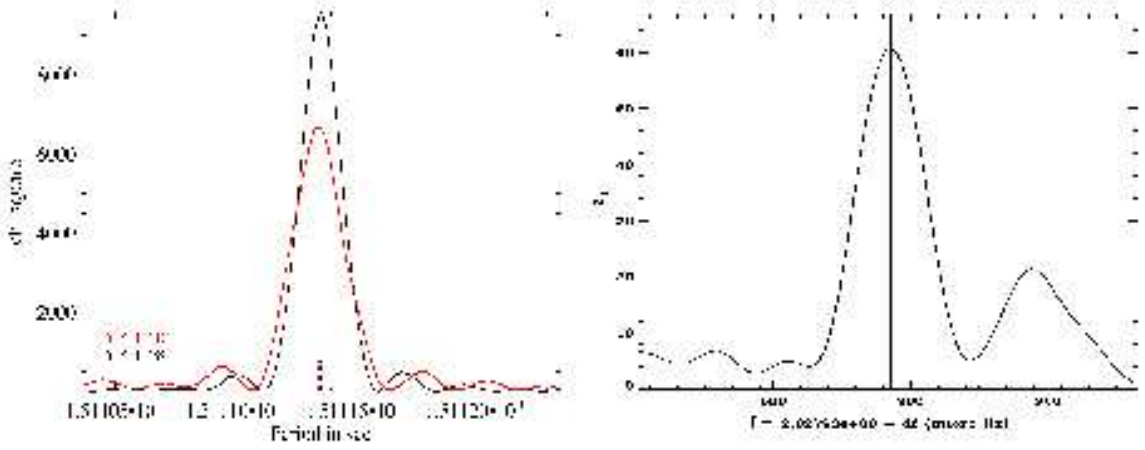

Figure 4: Left: Influence of a time jump of 31 s on the χ^2-distribution of epoch folding period search (pulsar period 150 ms). Red: time jump not detected. Black: time jump detected and corrected. The time jump causes broadening of the χ^2-distribution and increases the presence of secondary maxima.
Right: Influence of a time jump of 1 s on the Z^2-distribution of epoch folding period search (pulsar period 4 ms). The extrapolated radio period is indicated and agrees with the period found in the XMM-Newton data within the errors. A second major maximum appears.

Table 3: Summary of EPIC-pn time anomalies

anomaly	cause	signature	corrective action
spurious values in FTCOARSE	buffer overflow in electronics	FTCOARSE==32767	ignore as those frames are not associated with real event data
wrong FTCOARSE values for first frames after exposure start	reset pulse came too late	first FTCOARSE values are > 0	find first ok FTCOARSE value and approximate all preceding values (+FTFINE) by this good value minus integer multiple of nominal frame integration time
premature FTCOARSE increments	likely to be caused by ns-scale race condition in EPEA H/W; very rare	example FTCOARSE/FTFINE sequence: 5/42233 | 6/48828 | 6/6595 which should have been 5/42233 | 5/48828 | 6/6595	correct one affected FTCOARSE value by -1
random negative or positive jumps in FTCOARSE	unknown; bit-flips/SEU?, EPEA/EPDH sync problems?	time between consecutive events is negative or not an integer multiple of frame integration time; all subsequent FTCOARSEs are wrong until the next reset	adjust FTCOARSE value (and all subsequent ones until next reset) to make time difference integer multiple of nominal integration time
blocks of frames stemming from different quadrants	unknown - EPEA/EPDH, ODF generation?	the time jumps forward or backward by up to several seconds and some 10 frames later there is a jump in the opposite direction; most frequent jumps appear to be +1s/-7s	ignore frames from other quadrant

4. RELATIVE AND ABSOLUTE TIMING OF XMM-NEWTON

In the last year two critical points of the XMM-Newton timing accuracy have been solved. First, the relative timing could be improved up to the theoretically attainable accuracy. Second, the origin of the long standing issue of a shift in the absolute timing accuracy was located.

4.1 Relative Timing

The EPIC-pn camera was designed to offer outstanding time resolutions of down to 30 and 7 μs for Timing and Burst mode, respectively. This makes accurate timing studies, even on a ms-scale, feasible (cf. Becker and Aschenbach 2002)[9].

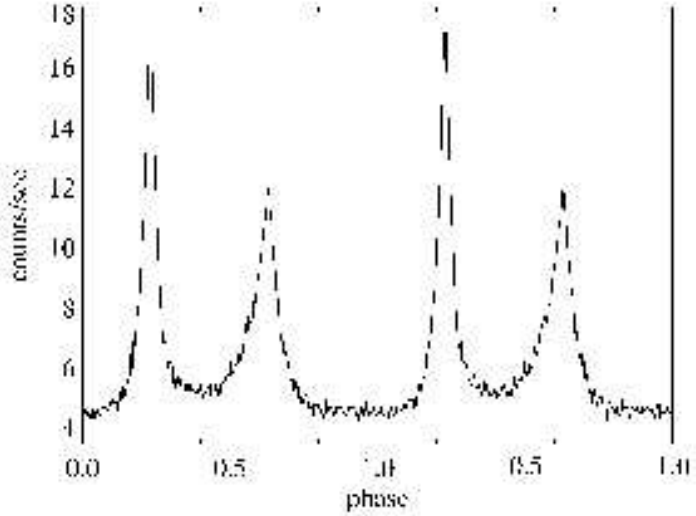

Figure 5: Pulse profile of the Crab-Pulsar of the 3 observations in rev. 411. 250 phase bins in the energy range from 0.6-15 keV were used. Two phase cycles are shown for clarity.

In the earlier SAS releases the true period of a periodic source could be only determined to one part in 10^{-6} due to a coding error in the task "*barycen*". The release of SAS 5.3 comprised for the first time all necessary components to support such timing analysis.

Tests on data from the Crab pulsar taken during XMM-Newton's performance verification campaign in early 2000 indicate that the relative deviation in the observed pulse period w.r.t. the most accurate radio data available is now considerably better than 10^{-8}. Furthermore a dedicated calibration campaign in revolution 411, where the Crab was observed at different periods of the orbit, shows even better results. The most accurate period for the Crab-Pulsar has been derived by using the epoch folding technique. The value for the period P was derived for the observations in revolutions 234 and 411 separately by using extrapolated data from the Jodrell Bank Crab Pulsar Monthly Ephemeris for P' (http://www.jb.man.ac.uk). The most accurate found X-ray periods from revolution 234 and 411 were 33.52130947 ms for epoch 51988.6405766415 (MJD) and 33.5341004590 ms for the 52340.6825136183 (MJD). Thus the relative deviation in the observed pulse period w.r.t. the most accurate radio data available ($\Delta P/P$) was less than some 10^{-9} (Kirsch 2003)[8].

For the Crab pulsar the new results now conform with estimates of the theoretically attainable accuracy with XMM-Newton and the expected statistical errors. Further investigations for periods of other objects are currently underway.

4.2 Absolute Timing

The various components in the time correlation process all have some uncertainties. Table 4 summarises the accuracy of the components:

Table 4: Accuracy of processes in time correlation

process	accuracy in micro s
Maximum drift in OBT between consecutive STSP	4
Maximum error in OBT distribution to users	11
Maximum error between latching OBT and start of frame transmission	9
Maximum error due to orbital uncertainties (10 km)	30
Maximum uncertainty in ground station delay	5
Maximum interpolation errors	10

This results in a theoretical overall accuracy of better than 100 µs. However, analysis on observations of the Crab pulsar with the EPIC-pn camera suggested till recently still a shift in absolute timing of the order of 1.2-1.5 ms. Becker and Aschenbach (2002)[9] found the X-ray pulse leading the radio pulse by ~1.5 ms. It was discovered very recently that this shift was caused by a wrongly corrected CDMU delay (626.17 µs). That delay was erroneously subtracted instead of added which accounted for a shift of 1252.34 µs.

The XMM-Newton absolute timing accuracy is now found to be in the range ~300-600 μs, based on the available calibration data. This is in agreement with Crab observations performed by RXTE and Chandra. Regular calibration measurements to monitor the absolute timing accuracy of the onboard clock will be performed throughout the mission.

Table 5: Summary of pulse arrival time measurements using the Crab data taken with XMM-Newton in 2000-2002. f_rad is the radio frequency (1/rotation period), f_xmm the frequency determined from the XMM-Newton data using a Z^2-search technique. MXP gives the phase location of the main X-ray peak in the Crab pulsars pulse profile. The radio peak is supposed to be at phase 0 or, equivalent, at phase 1, 1-MXP is the phase difference to the expected radio peak in units of phase angle and milliseconds.

		f_rad	f_xmm	MXP	1-MXP	1-MXP
Orbit	OBS ID	[Hz]	[Hz]	[phase]	[phase]	[ms]
56	0122330801	29.84375911	29.8437591143	0.98174	0.01830	0.60350
234	0135730701	29.83195269	29.8319526890	0.98723	0.01270	0.44256
411	0153750201	29.82015493	29.8201549266	0.98845	0.01150	0.40233
411	0153750301	29.82015493	29.8201549266	0.98910	0.01090	0.36210
411	0153750401	29.82015493	29.8201549266	0.98996	0.01000	0.32187
411	0153750501	29.82015493	29.8201549266	0.98989	0.01010	0.32187

5. EXAMPLE OF EPIC-PN TIMING ANALYSIS: XTEJ1807-294

The accreting millisecond pulsar XTE J1807-294, discovered by RXTE on February 21 (Markwardt et al. 2003)[10] was observed by XMM-Newton March 22, 2003 under ObsId 0157960l in revolution number 0601. The observation started on 2003-03-22T13:40:27Z. The EPIC pn-CCD camera was operated in Timing mode with the thick filter, while the two MOS cameras were in Small Window mode (MOS1) and Full Frame mode (MOS2). For this analysis only data from the 9.293 ks pn exposure were used. The count rate in 9 CCD columns (~ 37 arcsec) centred on the source was 33 cts/s in the 0.5-10 keV band (~ 3.7 mCrab). This compares to a background of 0.4 cts/s for a region of the same size.

Figure 6: Left: 0.5 to 10 keV pulse profile of single and double events of XTE J1807-294 from EPIC pn Timing mode. Right: Pulse profiles of XTE J1807-294 in three energy bands. Two phase cycles are shown for clarity.

Using the best-fit orbital period of 40.0741 ± 0.0005 minutes found by Markwardt et al. (2003)[11] we grouped the events into 20 phase bins of the binary orbit. χ^2-maximum epoch folding on individual phase bins revealed a clear modulation of the spin period. Assuming as a first approximation, a circular orbit, we derived 4.8 ± 0.1 light-ms for the projected

orbital radius. The barycentric mean spin period of the pulsar was found at 5.2459427 ± 0.0000004 ms. The modulation is seen over the entire energy band from 0.5 to 10 keV. The pulse profile shows a single peak (~ 1.5 ms FWHM), its shape varies only slightly with energy. The combined pulse profile in the 0.5-10 keV band shows a modulation of 6.0 ± 0.1 percent (90-percent confidence level) (Kirsch and Kendziorra 2003)[12].

6. TIMING CAPABILITIES OF THE OTHER XMM-NEWTON INSTRUMENTS

6.1 The Reflection Grating Spectrometer

The RGS's main function is high-resolution spectroscopy of comparatively bright objects. In its normal operational mode, CCD readouts take place every 570 ms offering useful timing information for many objects excluding the fastest X-ray pulsars. At typical detected count rates, integration times of a few thousand seconds or more are required to build enough statistics. In addition, it is also possible to operate the instrument to increase the time resolution to 15 ms per CCD at the expense of one spatial coordinate, although this so-called HTR mode has not been offered to the community at large because of increased sensitivity of this mode for background fluctuations and the limited number of objects whose study might benefit.

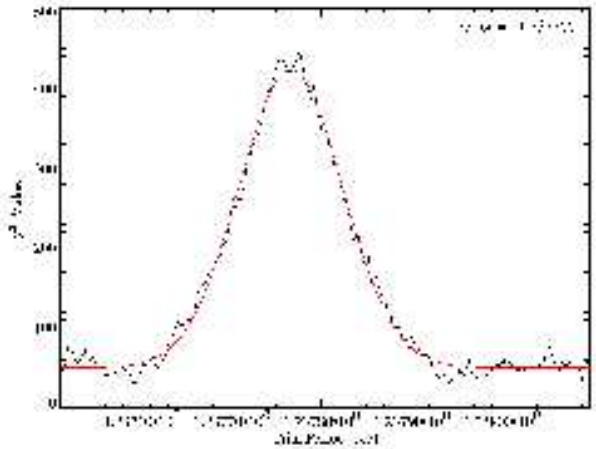

Figure 7: Results of an epoch-folding best period search on Her X-1 between 5 and 11 Angstroms.

Nonetheless, test observations of Her X-1 have been a success. Figure 7 shows an epoch-folding χ^2-period search on data between 5 and 11 Angstroms. The derived period is consistent with the period found by RXTE.

6.2 The Optical Monitor

The so-called Fast Mode of the Optical Monitor allows the user to perform fast photometry, with a maximum time resolution of 0.5 s, in any of its filters. Fast mode can be used only in a small window (10x10 arcsec^2) located anywhere within the OM field of view. Two of such windows can be commanded, allowing thus to perform differential photometry. Any of the six broad band filters, covering from the visible to the ultraviolet, can be used. A photon impinging into a fast mode window within the selected time slice (0.5 s minimum) is stored as an event with its arrival time and detector position. The XMM-Newton SAS will process the corresponding event list and a light curve will be produced.

This fast mode capability can be used to perform multi-wavelength (X-ray and optical to UV) observations of variable sources. Figure 8 (Mason et. al. 2002)[13] gives an example of such an application showing the simultaneous X-ray and UV light curves of the Low Mass X-ray Binary X1822-371.

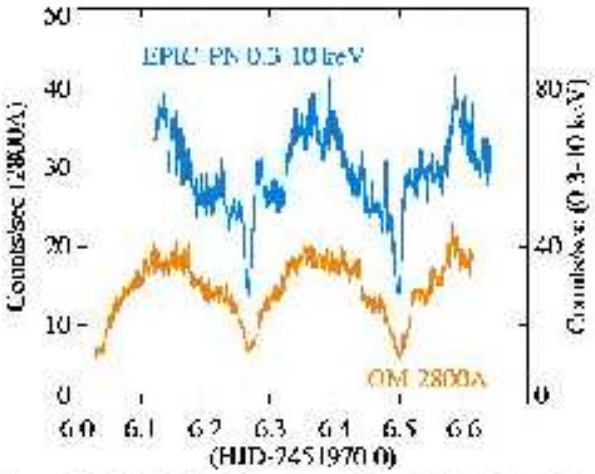

Figure 8: X1822-371 simultaneous X-ray (EPIC-PN) and UV light curve.

REFERENCES

1. E. Kendziorra et al, *PN-CCD camera for XMM: performance of high time resolution/bright source operating modes*, Proc. SPIE, 3114, 1997

2. E. Kendziorra et al., *Operational aspects of the PN-CCD camera for XMM-Newton and ABRIXAS*, Proc. SPIE 3765, 1999

3. M. Kuster et al., *Time resolution capability of the XMM EPIC pn-CCD in different readout modes* , Proc. SPIE 3765, 1999

4. M. Ehle et al., XMM-Newton Users Handbook, Issue 2.1, 2003

5. U.G. Briel, *Status of the calibration of the EPIC-pn-detector onboard XMM-Newton,* Proc. SPIE 5165 (this volume), 2003

6. M. G. F. Kirsch et al. (2002), *Calibration of the XMM-Newton EPIC-pn camera in the fast modes*, Proc. Symposium "New Visions of the X-ray Universe in the XMM-Newton and Chandra Era", ESA SP-488, eds. F. Jansen, 2002

7. E. Serpell and F. Possanzini, *XMM-Newton Time Correlation*, XMM-OPS-RP-0026-TOS-OF Issue 1, 2003

8. M. G. F. Kirsch, *In-Orbit-Kalibration der EPIC-pn-Kamera auf XMM-Newton in hoch zeitauflösenden Modes und Pulsphasenspektroskopie des Crab-Pulsars,* PhD thesis University of Tuebingen, ISBN 3-89959-070-8, 2003

9. W. Becker and B. Aschenbach, *X-ray Observations of Neutron Stars and Pulsars: First Results from XMM-Newton,* Proceedings of the 270. WE-Heraeus Seminar on Neutron Stars, Pulsars and Supernova Remnants, Jan. 21-25, 2002, Physikzentrum Bad Honnef, eds W. Becker, H. Lesch & J. Truemper, MPE-Report 278, 2002

10. C. B. Markwardt et al., IAUC 8080, 2003

11. C. B. Markwardt et al. , ATEL # 127, 2003

12. M. G. F. Kirsch and E. Kendziorra, ATEL # 148, 2003

13. K. Mason, Proc. Symposium "New Visions of the X-ray Universe in the XMM-Newton and Chandra Era", ESA SP-488, eds. F. Jansen, 2002